

ULTRA-LOW-DOSE NALOXONE SUPPRESSES OPIOID TOLERANCE, DEPENDENCE AND ASSOCIATED CHANGES IN MU OPIOID RECEPTOR–G PROTEIN COUPLING AND G $\beta\gamma$ SIGNALING

H.-Y. WANG,^{a*} E. FRIEDMAN,^a M. C. OLMSTEAD^b AND L. H. BURNS^c

^aDepartment of Physiology and Pharmacology, City University of New York Medical School, 138th Street and Convent Avenue, New York, NY 10031, USA

^bDepartment of Psychology, Queen's University, Kingston, Ontario, K7L 3N6 Canada

^cPain Therapeutics, Inc., 416 Browning Way, South San Francisco, CA 94080, USA

Abstract—Opiates produce analgesia by activating μ opioid receptor-linked inhibitory G protein signaling cascades and related ion channel interactions that suppress cellular activities by hyperpolarization. After chronic opiate exposure, an excitatory effect emerges contributing to analgesic tolerance and opioid-induced hyperalgesia. Ultra-low-dose opioid antagonist co-treatment blocks the excitatory effects of opiates *in vitro*, as well as opioid analgesic tolerance and dependence, as was demonstrated here with ultra-low-dose naloxone combined with morphine. While the molecular mechanism for the excitatory effects of opiates is unclear, a switch in the G protein coupling profile of the μ opioid receptor and adenylyl cyclase activation by G $\beta\gamma$ have both been suggested. Using CNS regions from rats chronically treated with vehicle, morphine, morphine+ultra-low-dose naloxone or ultra-low-dose naloxone alone, we examined whether altered μ opioid receptor coupling to G proteins or adenylyl cyclase activation by G $\beta\gamma$ occurs after chronic opioid treatment. In morphine-naïve rats, μ opioid receptors coupled to G α_o in striatum and to both G α_i and G α_o in periaqueductal gray and spinal cord. Although chronic morphine decreased G α_o coupling by μ opioid receptors, a pronounced coupling to G α_s emerged coincident with a G $\beta\gamma$ interaction with adenylyl cyclase types II and IV. Co-treatment with ultra-low-dose naloxone attenuated both the chronic morphine-induced G α_s coupling and the G $\beta\gamma$ signaling to adenylyl cyclase, while increasing G α_o coupling toward or beyond vehicle control levels. These findings provide a molecular mechanism underpinning opioid tolerance and dependence and their attenuation by ultra-low-dose opioid antagonists. © 2005 IBRO. Published by Elsevier Ltd. All rights reserved.

Key words: morphine, antinociception, withdrawal, signal transduction, adenylyl cyclase.

*Corresponding author. Tel: +1-212-650-8813; fax: +1-212-650-7726. E-mail address: hywang@sci.cuny.cuny.edu (H.-Y. Wang).
Abbreviations: [³H]DAMGO, Tyr-D-Ala-Gly-N-Methyl-Phe-Gly; GIRK channels, G protein-activated inwardly rectifying potassium channels; KOR, κ opioid receptor; MOR, μ opioid receptor; NLX, naloxone; PAG, periaqueductal gray; PBST, PBS with 0.1% Tween-20; PMSF, phenylmethylsulfonyl fluoride; VDCC, voltage-dependent calcium channel.

Mu opioid receptors (MORs) preferentially couple to pertussis toxin-sensitive G proteins, G α_i and G α_o , to inhibit the adenylyl cyclase/cAMP pathway (Laugwitz et al., 1993; Connor and Christie, 1999). The analgesic effects of MOR activation have been predominantly attributed to the G $\beta\gamma$ dimer released from G α_o , which activates G protein-activated inwardly rectifying potassium (GIRK) channels (Ikeda et al., 2000) and inhibits voltage-dependent calcium channels (VDCCs) (Saegusa et al., 2000), thereby suppressing cellular activities by hyperpolarization. Adenylyl cyclase inhibition may also contribute to opioid analgesia, or its activation may contribute to analgesic tolerance, since overexpression of adenylyl cyclase type 7 in the CNS of mice leads to more rapid tolerance to morphine (Yoshimura et al., 2000). Additionally, adenylyl cyclase activation has been suggested to elicit analgesic tolerance or tolerance-associated hyperalgesia (Wang and Gintzler, 1997). Although the superactivation of adenylyl cyclase after chronic opioid administration is more often viewed as a hallmark of opioid dependence than as a mediator of tolerance (Nestler, 2001), both are consequences of chronic opioid administration, and tolerance often worsens dependence. Chronic pain patients who have escalated their opioid dose over time often experience more withdrawal than patients on a constant dose.

While the cellular effects of opiates are normally inhibitory, several *in vitro* studies have demonstrated that opiates can elicit excitatory effects either at low doses (Shen and Crain, 1989; Crain and Shen, 1990) or after chronic exposure (Crain and Shen, 1992). *In vivo*, opiates can cause “paradoxical hyperalgesia” at low doses (Kayser et al., 1987; Kiyatkin, 1989; Crain and Shen, 2001), or after chronic administration, opioid-induced hyperalgesia (Arner et al., 1988). While descending facilitation of spinal cord dorsal horn neurons has been implicated in tolerance-associated hyperalgesia (Vanderah et al., 2001), alterations in opioid receptor signaling also occur (Shen and Crain, 1989; Crain and Shen, 1990, 1992; Gintzler and Chakrabarti, 2001) and may contribute to the enhanced firing of descending brainstem projections. Co-administration of an ultra-low-dose opioid antagonist blocks the excitatory effects of opiates *in vitro* and apparent behavioral manifestations: tolerance, withdrawal signs and hyperalgesia associated with tolerance or low doses of opiates (Crain and Shen, 1995, 2001; Shen and Crain, 1997). These findings suggest that excitatory effects of opiates underlie tolerance, dependence and “paradoxical hyperalgesia.”

One proposed mechanism of excitatory effects of opiates is a switch in G protein coupling by opioid receptors (Shen and Crain, 1990). A switch in G protein coupling from Gi/o to Gs would activate rather than inhibit adenylyl cyclase, and may also alter the usual G $\beta\gamma$ signaling to GIRK channels and VDCCs. Alternatively, excitatory signaling of opioid receptors may also occur by G $\beta\gamma$ activation of adenylyl cyclase (Wang and Gintzler, 1997; Gintzler and Chakrabarti, 2001). Data derived from blocking Gs by cholera toxin or Gi/o by pertussis toxin suggested that low doses of opiates may elicit excitatory effects via Gs, but that opioid tolerance is instead mediated by G $\beta\gamma$ stimulation of adenylyl cyclase (Wang and Gintzler, 1997). Adenylyl cyclase types II and IV can be activated by G $\beta\gamma$ (Fedorin et al., 1992) including the G $\beta\gamma$ associated with MOR, yet the adenylyl cyclase superactivation underlying opioid dependence does not appear to involve these enzyme subtypes (Avidor-Reiss et al., 1995). However, an enhanced activation of adenylyl cyclases II and IV by MOR stimulation could counteract opioid analgesia, contributing to tolerance.

This work is the first to directly assess the interaction between MOR and Gs proteins as well as coupling between MOR-associated G $\beta\gamma$ and adenylyl cyclase in opioid tolerance *in vivo*. Ultra-low-dose naloxone (NLX) co-treatment was used to alleviate morphine antinociceptive tolerance and physical dependence, and the effects of this ultra-low-dose opioid antagonist co-treatment on these G protein interactions associated with the MOR were also assessed.

EXPERIMENTAL PROCEDURES

Animals and drug treatments

Pathogen-free, male 225–250 g Sprague–Dawley rats (Taconic, Germantown, NY, USA) or Long Evans rats (Charles River, Saint-Constant, Quebec, Canada) were maintained on a 12-h light/dark cycle with free access to food and water. All animal procedures were in compliance with the National Institutes of Health *Guide for Care and Use of Laboratory Animals* and were approved by the Animal Care and Use Committees of City College of New York and Queen's University, Kingston, ON for respective procedures. Animals used were an estimated minimal number required for meaningful statistics.

For molecular pharmacology experiments, four treatment groups of four rats each received s.c. injections of saline (control), morphine (10 mg/kg), the combination of morphine (10 mg/kg) plus NLX (10 ng/kg) or 10 ng/kg NLX twice daily for 7 days. These animals were killed by decapitation 16 h after the last injection, and dorsal striatum, periaqueductal gray (PAG) and thoracic spinal cord regions were harvested on ice immediately. Behavioral experiments included eight rats/group, and dose groups were the same but excluded a vehicle group. All behavioral testing/scoring was performed by a rater blind to drug treatments.

Antinociception

The tail-flick test was used to assess nociceptive thresholds to a painful heat stimulus. The apparatus consisted of a digital analgesia meter with a projection lamp as the heat source. Light from the lamp is aimed at a photocell 25 cm above the lamp, and both the lamp and timer are turned off when the tail moves out of the light beam. To minimize stress-induced analgesia, animals were

habituated for 5–10 min on the apparatus one day prior to testing. For testing, animals were placed on the apparatus and the light sensor and heat source are aimed at the middle third of the tail. Once set, the heat source was turned on, and the latency to remove the tail recorded. The heat intensity was adjusted to yield a 5 s baseline response, and a cutoff time of 10 s was implemented to minimize tissue damage. A baseline antinociception test preceded drug administration, and subsequent tests occurred 30 min after the a.m. dose on days 1, 3, 5 and 7 of drug administration.

Withdrawal testing

On day 8, 16–20 h after the last drug injection, animals were given NLX to precipitate withdrawal (1 mg/kg, s.c.) before being placed in an observation chamber for 1 h. A scale adapted from MacRae and Siegel (1997) was used to quantify four categories of withdrawal behaviors: wet dog shakes, paw tremors, mouth movements, and ear wipes. Scores are summed to yield a total withdrawal score across the 1-h test.

MOR–G protein coupling

To determine the profile and magnitude of G protein coupling to MOR, four separate co-immunoprecipitation experiments were performed for both striatum and spinal cord, each using membranes prepared from one rat from each treatment group. For each of these four experimental runs, membranes were incubated *in vitro* with either Krebs–Ringer or 1 μ M morphine and then solubilized. The obtained lysates were divided for separate passage through immunoaffinity columns containing immobilized antibodies to G α s/olf, G α i, G α o or G α q/11 to purify specific G protein-associated MORs, which were subsequently detected by Western blotting. The key findings of MOR–Gs coupling following chronic morphine treatment and reduction by NLX co-treatment have also been replicated with five different rats per treatment group in a separate experiment of a different experimental design (Wang et al., 2004b).

Enriched synaptic membranes (200 μ g) were incubated with 1 μ M morphine for 5 min at 37 °C in Krebs–Ringer solution. Membranes were solubilized in immunoprecipitation buffer (25 mM HEPES, pH 7.5; 200 mM NaCl, 2 mM MgCl₂, 1 mM EDTA, 0.2% 2-mercaptoethanol, 50 μ g/ml leupeptin, 25 μ g/ml pepstatin A, 0.01 U/ml soybean trypsin inhibitor, 0.04 mM phenylmethylsulfonyl fluoride [PMSF]) containing 0.5% digitonin, 0.2% sodium cholate and 0.5% NP-40 at 4 °C with end-over-end shaking for 60 min. After centrifugation at 50,000 \times g for 5 min to remove insoluble debris, the obtained supernatant was used to assess MOR–G protein coupling by co-immunoprecipitation of MOR and G proteins. The protein concentrations in supernatant were determined using the Bradford method according to manufacturer's instructions (Bio-Rad Laboratories, Hercules, CA, USA).

G protein-coupled MOR was immunopurified together with its associated G protein using immobilized anti-G α antibodies (20 μ g/column) to prevent interference from immunoglobulins. Anti-G α antibodies (Santa Cruz Biotechnology, Santa Cruz, CA, USA) were covalently cross-linked to protein-G-conjugated resin in Seize-X protein G immunoprecipitation kit (Pierce-ENDORGEN, Rockford, IL, USA) according to the manufacturer's instructions. MOR–G protein complexes in solubilized brain lysates were isolated by immunoprecipitation in which 200 μ g solubilized brain membrane extracts were incubated with immobilized anti-G α -protein G-resin at 4 °C overnight. After centrifugation and three washes with phosphate-buffered saline (pH 7.2) at 4 °C, the MOR–G protein complexes were eluted with 200 μ l of antigen elution buffer (pH 2.8). The obtained eluate was neutralized immediately by addition of 20 μ l of 1.5 M Tris buffer (pH 8.8). To achieve complete solubilization of the obtained proteins, the neutralized eluate was combined with 180 μ l of 2 \times PAGE sample

preparation buffer (62.5 mM Tris–HCl, pH 6.8; 20% glycerol, 4% SDS; 10% 2-mercaptoethanol, 0.1% Bromophenol Blue) and boiled for 5 min. The level of specific G protein-associated MORs in the anti-G α column eluate was determined by Western blotting using a specific antibody directed against the amino-terminal region of the MOR (Santa Cruz Biotechnology). A control experiment that used a specific antibody against the κ opioid receptor (KOR, Santa Cruz Biotechnology) to assess both MOR and KOR–G protein coupling in both wild-type and MOR knockout mice demonstrated minimal cross-reactivities between antibodies against MOR and KOR.

To achieve a complete elution of antigens from the G α immunocomplexes, a highly acidic elution buffer (pH 2.8) was used. Because this elution procedure yielded MOR with an approximate molecular weight of 53 kDa that appears to be the de-glycosylated form of MOR, we compared elution by this highly acidic antigen elution buffer to an elution with a neutral pH. Acid treatment has previously been shown to de-glycosylate proteins (Veerman et al., 1995). While the acidic buffer completely de-glycosylated MORs to yield a protein of 53 kDa, eluting with the neutral pH buffer yielded predominantly MORs with an apparent molecular weight of 67 kDa (Fig. 1). This control experiment demonstrated that the anti-MOR antibody recognizes a 67-kDa form of the receptor that is the functional, glycosylated form of the receptor (Chen et al., 1995). This conclusion was also supported by the demonstration that specific [3 H]DAMGO (Tyrd-Ala-Gly-N-Methyl-Phe-Gly) binding was readily detected in the neutral pH eluate (data not shown).

The specificity of the four anti-G α antibodies was determined by Western blotting using 100 μ l of anti-G α column eluate with specific anti-G α antibodies with or without antigen peptide (25 μ g) pre-adsorption for 30 min. All four anti-G α antibodies were specific in purifying the intended G α protein except for a minor cross-reactivity to G α o by anti-G α i (Fig. 2). Specificity is further supported by the fact that pre-adsorption with 25 μ g of their respective antigen peptides drastically weakened or abolished the detection of targeted G α proteins.

In a confirmatory set of experiments with spinal cord tissue, MORs that co-immunoprecipitated with G α proteins were quantified by a [3 H]DAMGO binding assay. Anti-G α –G protein–MOR complexes were washed three times with 1 ml phosphate-buffered saline (PBS), pH 7.2, and collected by centrifugation at 4 $^{\circ}$ C. MOR binding was assayed in washed pellets that were suspended in 500 μ l binding buffer containing 50 mM Tris–HCl, pH 7.5, 5 mM MgCl $_2$, 50 μ g/ml leupeptin, 25 μ g/ml pepstatin A, 0.01 U/ml soybean trypsin inhibitor, 0.04 mM PMSF. The suspension was incubated at 30 $^{\circ}$ C for 30 min with 2 nM [3 H]DAMGO (51 Ci/mmol, PerkinElmer Life and Analytical Sciences, Boston, MA, USA). Non-specific binding was defined by 10 μ M NLX and consisted of approximately 10% of total [3 H]DAMGO binding. The reactions were terminated by filtering through 10-kDa molecular weight cutoff filters (Cole-Parmer Instruments). After three washes of the filters with 5 ml of ice-cold washing buffer (50 mM Tris–HCl, pH 7.5), the amount of radioactivity trapped on the filters was determined by liquid scintillation spectrometry. To confirm that DAMGO binding sites are indeed the functional MORs recognized by anti-MOR and further address the specificity of the various antibodies to various opioid receptor subtypes, [3 H]DAMGO was incubated with anti-MOR, δ or κ -KOR immunoprecipitates. While the anti-MOR immunoprecipitate contained specific [3 H]DAMGO binding sites, a negligible amount of [3 H]DAMGO was detected in immunoprecipitates of anti- δ or κ -KOR antibodies (Santa Cruz Biotechnology, data not shown).

DAMGO-induced [35 S]GTP γ S binding to G α proteins

PAG tissue was homogenized in 10 volumes of ice cold 25 mM HEPES buffer, pH 7.4, which contained 1 mM EGTA, 100 mM sucrose, 50 μ g/ml leupeptin, 0.04 mM PMSF, 2 μ g/ml soybean trypsin inhibitor and 0.2% 2-mercaptoethanol. The homoge-

nates were centrifuged at 800 \times g for 5 min and the supernatants were centrifuged at 49,000 \times g for 20 min. The pellets were suspended in 10 volume of reaction buffer, which contained 25 mM HEPES, pH 7.5, 100 mM NaCl, 50 μ g/ml leupeptin, 2 μ g/ml soybean trypsin inhibitor, 0.04 mM PMSF and 0.2% 2-mercaptoethanol. The resultant PAG membrane preparation (200 μ g) was incubated at 30 $^{\circ}$ C for 5 min in reaction buffer that contained 1 mM MgCl $_2$ and 0.5 nM [35 S]GTP γ S (0.1 μ Ci/assay, PerkinElmer Life and Analytical Sciences) in a total volume of 250 μ l. Incubation continued for 5 min in the absence or presence of 1 μ M DAMGO. The reaction was terminated by dilution with 750 μ l of ice-cold reaction buffer that contained 20 mM MgCl $_2$ and 1 mM EGTA and immediate centrifugation at 16,000 \times g for 5 min. The resulting pellet was solubilized in 0.5 ml of immunoprecipitation buffer containing 0.5% digitonin, 0.2% sodium cholate and 0.5% NP-40. Solubilization was facilitated by sonication for 10 s. Normal rabbit serum (1 μ l) was added to 1 ml of lysate and incubated at 25 $^{\circ}$ C for 30 min. Nonspecific immune complexes were removed by incubation with 25 μ l of protein A/G-conjugated agarose beads at 25 $^{\circ}$ C for 30 min followed by centrifugation at 5000 \times g at 4 $^{\circ}$ C for 5 min. The supernatant was divided and separately incubated for 30 min at 25 $^{\circ}$ C with four specific G α protein antibodies (1:1000 dilution). The anti-G α immune complexes were collected by incubation for 30 min at 25 $^{\circ}$ C with 40 μ l of agarose-conjugated protein A/G beads and centrifugation at 5000 \times g at 4 $^{\circ}$ C for 5 min. The pellet was washed and suspended in buffer containing 50 mM Tris–HCl, pH 8.0, and 1% NP-40. The radioactivity in the suspension was determined by liquid scintillation spectrometry. The binding of [35 S]GTP γ S to G α proteins is specific since 100 nM GTP γ S or Gpp(NH)p completely abolished [35 S]GTP γ S in G α immunoprecipitates (data not shown).

DAMGO-stimulated coupling of G $\beta\gamma$ to adenylyl cyclase type II or IV

Types II and IV adenylyl cyclases are activated by G $\beta\gamma$ that results from the dissociation of G proteins following receptor stimulation. This set of experiments assessed whether adenylyl cyclase type II or IV couples to G $\beta\gamma$ after stimulation of MOR. Two hundred micrograms of the synaptic membranes prepared from the CNS regions of interest were incubated with 1 μ M DAMGO in the presence of 1 nM Gpp(NH)p for 5 min at 37 $^{\circ}$ C (Friedman and Wang, 1996). The addition of the non-hydrolyzable Gpp(NH)p prevents re-association of the dissociated G $\beta\gamma$ with G α -Gpp(NH)p. Membranes were solubilized in immunoprecipitation buffer containing 0.5% digitonin, 0.2% sodium

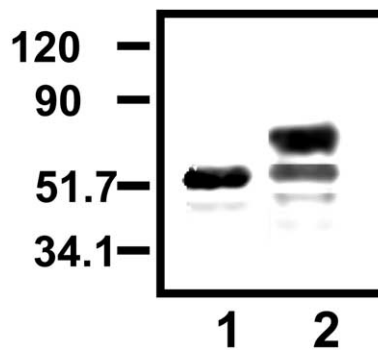


Fig. 1. Molecular weight of MOR immunoprecipitated by the anti-MOR antibody after elution with an acidic versus a neutral buffer. Elution with the highly acidic (pH 2.8) antigen elution buffer yielded MORs with an apparent molecular weight of 53 kDa (lane 1). Elution with a neutral pH gentle elution buffer yielded predominantly the glycosylated 67 kDa form with minor 53 kDa MOR proteins (lane 2).

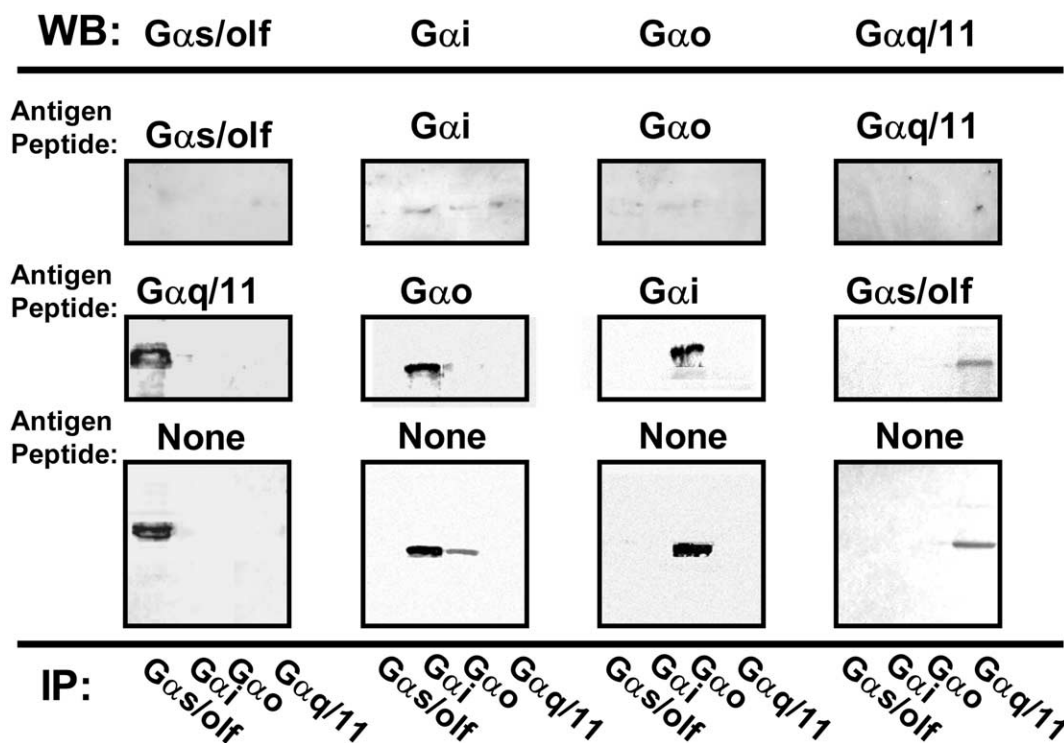


Fig. 2. Antibodies directed against Gαi, Gαo, Gαq/11 and Gαs/olf are specific to respective targeted Gα proteins. The specificities of the different anti-Gα antibodies were evaluated using the column eluates derived from immunoaffinity columns of covalently immobilized anti-Gαs/olf, -Gαi, -Gαo, or -Gαq/11 by quadruplicate Western blots probed respectively with these same four antibodies [bottom blots]. The blots were stripped and re-probed with these same four antibodies that were pre-absorbed for 30 min at 25 °C with 25 μg of non-matching antigen peptides (Gαq/11, Gαo, Gαi, and Gαs/olf, respectively incubating with anti-Gαs/olf, -Gαi, -Gαo, and -Gαq/11 antibodies) [middle blots]. The blots were stripped once again and re-probed with the four antibodies after they were pre-absorbed with 25 μg of respective antigen peptides for 30 min at 25 °C (Gαs/olf, Gαi, Gαo, Gαq/11 respectively incubating with anti-Gαs/olf, -Gαi, -Gαo, and -Gαq/11 antibodies) [top blots]. Despite a mild cross-reactivity of the anti-Gαi with Gαo that was eliminated by pre-adsorption with Gαo antigen peptide, all four anti-Gα antibodies specifically recognized their targeted Gα proteins. The specificity of these anti-Gα antibodies was further supported by the demonstration that pre-adsorption with the respective antigen peptides markedly reduced or abolished detection of the intended Gα protein.

cholate and 0.5% NP-40 at 4 °C with end-over-end rotation, and Gβγ was isolated by immunoprecipitation with an anti-panGβ antibody (2 μg). The adenylyl cyclase-Gβγ complexes in the anti-Gβ immunoprecipitates were recovered by centrifugation at 4 °C and the immunoprecipitates were washed three times with 1 ml PBS and solubilized by boiling for 5 min in 200 μl of PAGE sample preparation buffer. The levels of adenylyl cyclase subtypes in the anti-Gβ immunoprecipitates were assessed by Western analyses using specific antibodies directed against adenylyl cyclase II and IV subtypes. These experiments used membrane preparations from striatum and spinal cord.

The specificities of these antibodies for adenylyl cyclase II or IV were demonstrated using 100 μl of eluates derived from covalently immobilized anti-adenylyl cyclase I, II, IV or V columns (Fig. 3).

Western blot analysis

Striatal, spinal cord and PAG membranes were prepared as described above and protein concentration was determined by the Bradford method. Membranes were solubilized by boiling for 5 min in SDS-PAGE sample preparation buffer. A 20-μg aliquot of solubilized membranes was separated by 12% SDS-PAGE and electrophoretically transferred to nitrocellulose membranes. The membranes were washed with PBS and blocked overnight at 4 °C with 10% milk followed by washing with PBS with 0.1% Tween-20 (PBST) and incubation at room temperature for 2 h with antibodies against specific Gα proteins (separately, at 1:1000 dilutions) and anti-MOR antibodies (1:500 dilution). After washing, membranes were incubated for 1 h with anti-rabbit IgG-HRP (1:5000 dilution) and washed

with 0.3% PBST followed by washing with 0.1% PBST. Immunoreactivity was visualized by reacting with ECL reagent (Pierce-ENDOGEN) for exactly 5 min and immediately exposing to X-ray film.

Specific bands were quantitated by densitometric scanning (GS-800 calibrated densitometer, Bio-Rad Laboratories). The contrast of each blot was adjusted based on the weakest band discernible from background. The optical densities of each band were then determined by subtracting the surrounding background. With the contrast adjusted equally to all bands in the blot, the optical density reflects the relative intensities of the bands.

Statistical analysis

All data are presented as mean ± standard error from the mean. Protein levels in Western blots were analyzed using optical intensities derived from densitometric scans. Treatment effects were evaluated by two-way ANOVA followed by Newman-Keul's test for multiple comparisons. Two-tailed Student's *t*-test was used for post hoc pairwise comparisons. The threshold for significance was $P < 0.05$.

RESULTS

Ultra-low-dose NLX prevents morphine antinociceptive tolerance and dependence

Rats treated with morphine (10 mg/kg)+NLX (10 ng/kg) showed no antinociceptive tolerance over the 7 days of drug administration in contrast to rats treated with morphine alone (Fig. 4A). In fact, a ceiling effect in the

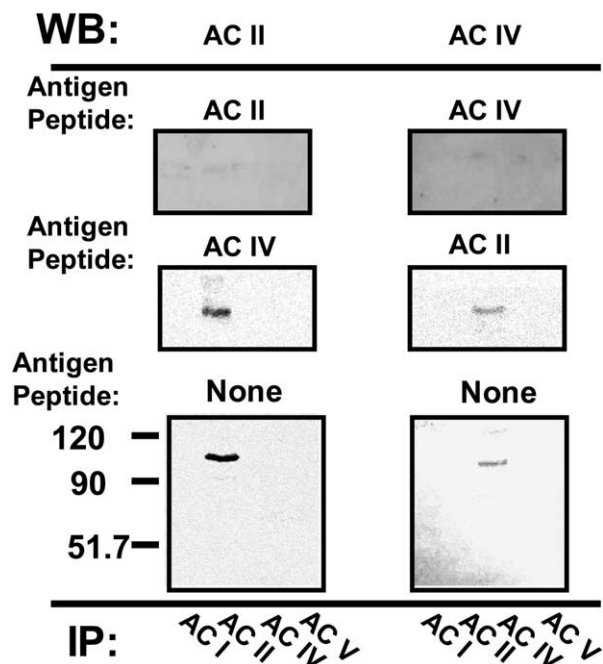


Fig. 3. Antibodies directed against adenylyl cyclase type II and IV are specific to these respective adenylyl cyclase subtypes. The specificities of antibodies to adenylyl cyclase type II (AC II) and adenylyl cyclase type IV (AC IV) were evaluated using the column eluates derived from immunoaffinity columns of the covalently immobilized anti-AC I, -AC II, -AC IV and -AC V antibodies by Western blotting with specific anti-AC II and -AC IV antibodies [bottom blots]. The blots were stripped and re-probed with these same two antibodies that this time were pre-absorbed for 30 min at 25 °C with 25 μ g of the alternate antigen peptide (i.e. anti-AC II and anti-AC IV were pre-absorbed respectively with AC IV and AC II peptides) [middle blots]. The blots were stripped once again and re-probed with 25 μ g of their respective antigen peptides for 30 min at 25 °C [top blots]. The data demonstrate that both anti-AC II and anti-AC IV are specific to their targeted AC subtype. The specificity of these anti-G α antibodies was clarified further by the demonstration that pre-adsorption with the respective antigen peptides nearly abolished the detection of intended AC subtype.

morphine+NLX group on days 5 and 7 suggests a slight augmentation of antinociception over the week of testing. ANOVA revealed a significant effect of treatment ($P<0.01$) and a significant treatment \times time interaction ($P<0.01$). Treatment with NLX alone had no antinociceptive effect, as latencies for this group did not differ from baseline on any day of testing. While morphine+NLX produced a significant antinociceptive effect compared with the NLX alone group ($P<0.05$) on all days, the antinociceptive effect of morphine alone declined over the testing period to a level not significantly different from NLX alone (compared with NLX alone: day 1, $P<0.01$; day 3, $P<0.01$; day 5, $P<0.05$; day 7, N.S.). Tail-flick latencies for the morphine+NLX group were significantly longer than those of the morphine group on days 3, 5 and 7 ($P<0.01$).

The addition of 10 ng/kg NLX to morphine also significantly reduced signs of physical dependence seen in rats chronically treated with morphine alone ($P<0.05$; Fig. 4B). Although the co-treatment completely blocked antinociceptive tolerance, the addition of ultra-low-dose NLX did not

fully block opioid dependence since withdrawal scores for the morphine+NLX group and the NLX only group were also significantly different ($P<0.05$).

Co-immunoprecipitation of MOR-G protein complexes shows that NLX attenuates Gs coupling

To determine whether alterations in MOR-G protein coupling mediate the excitatory signaling that occurs during opioid tolerance and whether ultra-low-dose opioid antagonists have any effect on such changes, we isolated MOR-express-

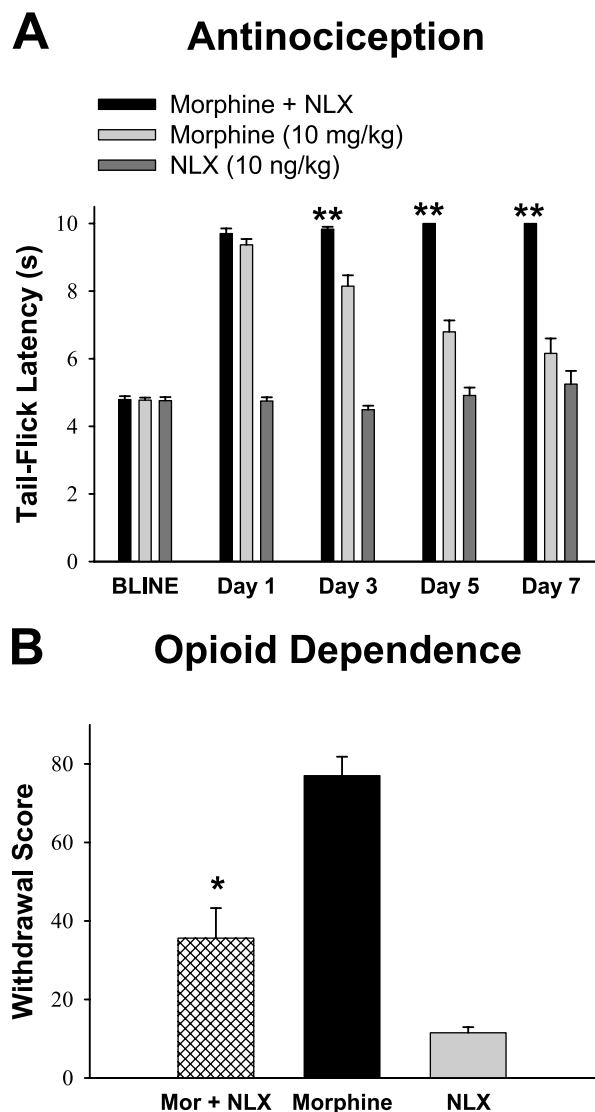


Fig. 4. Co-treatment with ultra-low-dose NLX (10 ng/kg) significantly prevented both the antinociceptive tolerance and the physical dependence associated with chronic morphine (10 mg/kg, s.c., twice daily for 7 days). Rats treated with morphine+NLX showed stable tail-flick latencies over the week of drug treatment, while tail-flick latencies of rats receiving morphine alone declined to a level not significantly different from NLX alone by day 7 (A). In a test of NLX-precipitated withdrawal, withdrawal scores of the morphine+NLX group were significantly lower than those of the morphine only group (B). Data are means \pm S.E.M. ($n=8$). * $P<0.05$ and ** $P<0.01$ for morphine+NLX vs. morphine. BLINE, pre-drug baseline.

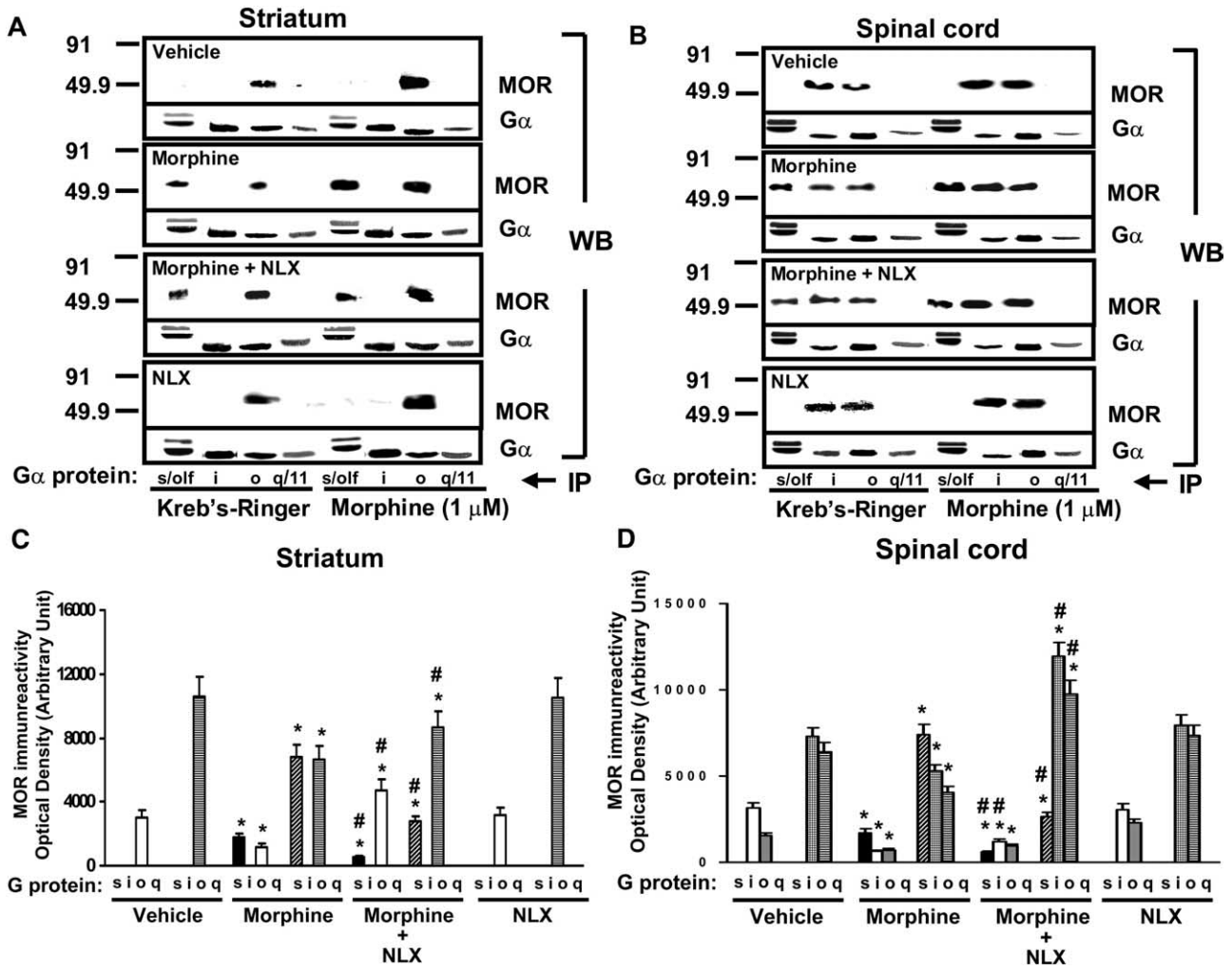


Fig. 5. Chronic morphine-induced Gs–MOR coupling is attenuated by co-treatment with ultra-low-dose NLX as demonstrated by co-immunoprecipitation of Gα proteins with MOR using specific anti-Gαs/olf (s/olf), -Gαi (i), -Gαo (o) or Gαq/11 (q/11) antibodies. MOR protein is detected in immunoprecipitates of Gαo and Gαs of striatum (A) or Gαi, Gαo and Gαs of spinal cord (B) from rats treated twice daily for 7 days with saline, morphine (10 mg/kg, s.c.), morphine+NLX (10 ng/kg, s.c.) or NLX (10 ng/kg, s.c.). The blots were stripped and re-probed with antibodies against various Gα proteins, demonstrating similar amounts of Gα protein precipitated regardless of *in vitro* morphine exposure or *in vivo* treatments. Densitometric quantifications of blots are shown in C and D. Data are means±S.E.M. derived from four individual rats in each of the treatment groups that were processed individually (*n*=4). Solid bars indicate basal coupling, and hatched bars indicate coupling after receptor stimulation by *in vitro* morphine. * *P*<0.05 versus same Gα protein in vehicle and NLX-treated groups. # *P*<0.05 versus same Gα protein in morphine group. For both regions, morphine-stimulated coupling was significantly greater (*P*<0.01) than basal coupling of each Gα protein within each treatment group.

ing CNS tissue from rats receiving twice daily s.c. injections of vehicle, 10 mg/kg morphine, 10 mg/kg morphine+10 ng/kg NLX or 10 ng/kg NLX for 7 days. This maximally analgesic dose of morphine resulted in analgesic tolerance in our behavioral experiment, as previously established (Yamamoto et al., 1988). Under non-denaturing conditions that keep MOR–G protein complexes intact, specific G proteins (Gi, Go, and Gs) together with their coupled receptors were immunoprecipitated with selective anti-Gα antibodies from solubilized synaptic membranes obtained from striatum or spinal cord of the four different treatment groups (*n*=4), under both basal and morphine-stimulated conditions. As receptor stimulation is known to recruit G proteins (Jin et al., 2001), *in vitro* morphine stimulation consistently increased MOR–G protein coupling well above basal levels, although an identical pat-

tern of MOR–G protein coupling was observed under both conditions.

The relative amounts of MORs coupling to each of the G protein subtypes in the four treatment groups are shown in Western blots of the Gα immunoprecipitates probed with the MOR-specific antibody (Fig. 5). In striatum, MOR coupled exclusively to Go in vehicle- and NLX-treated rats, and to both Go and Gs in morphine-treated rats. The Go coupling, however, was decreased in the chronic morphine group compared with the vehicle group (Fig. 5A and 5C). In striatum of rats treated with morphine+NLX, coupling to Gs was markedly decreased from that in the morphine-treated animals, whereas coupling to Go was increased toward control levels (Fig. 5A and 5C). In spinal cord of vehicle- and NLX-treated rats, MOR coupled to both Go and Gi, demonstrating a clear regional difference in

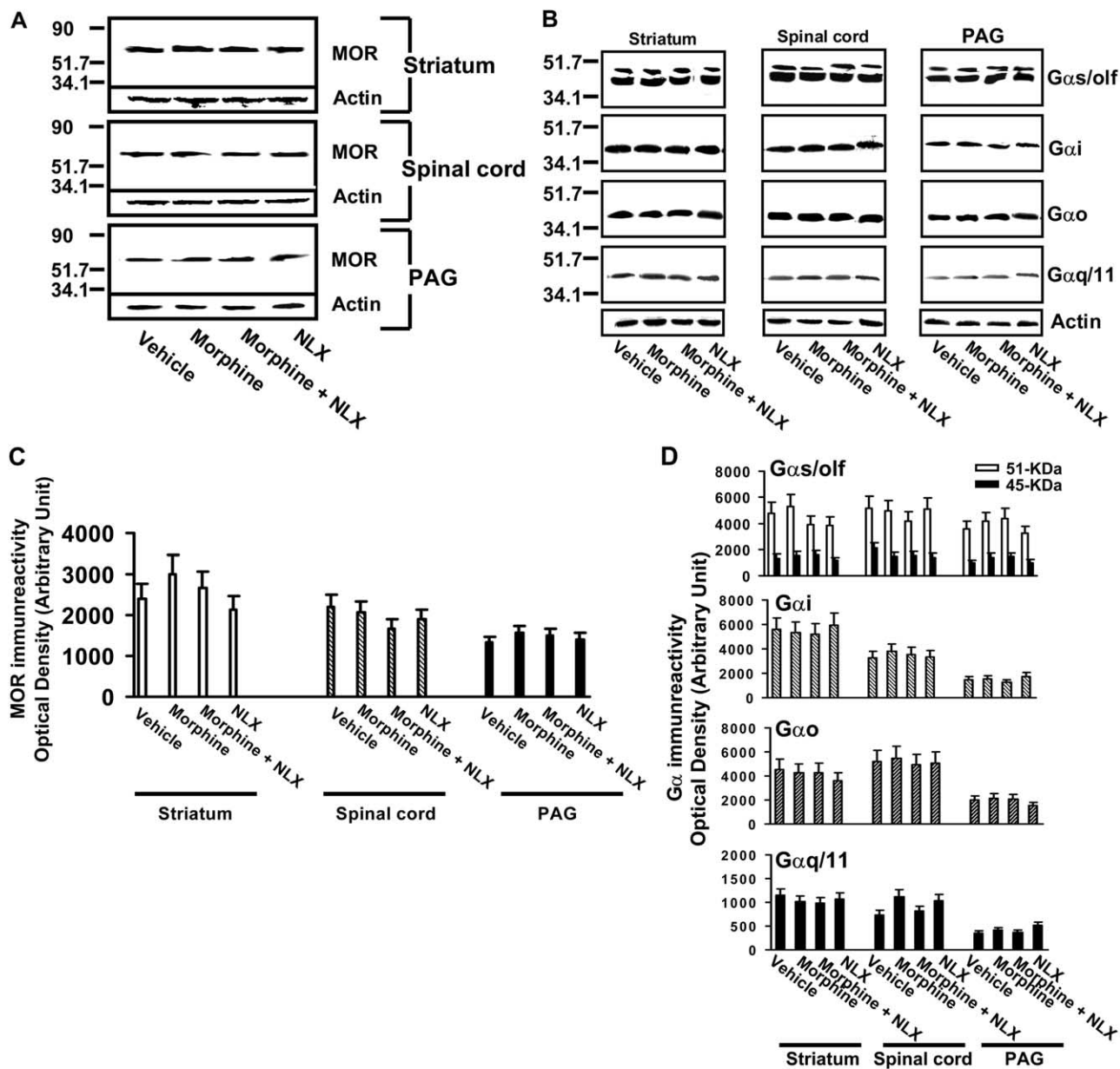


Fig. 6. Comparison of relative levels of MOR (A) and G α proteins (B) in the different treatment groups by Western blotting. The blots were stripped and re-probed with an anti-actin antibody to determine the actin immunoreactivities as loading controls. Densitometric quantifications of blots are shown in C and D. Alterations in G protein coupling induced by morphine and alleviated by ultra-low-dose NLX were not due to changes in expression of MOR or G α proteins in striatum, spinal cord or PAG as MOR and G α proteins levels were comparable between treatment groups in all brain areas examined. Data are means \pm S.E.M. derived from four individual rats in each treatment group that were processed individually ($n=4$).

MOR–G protein coupling profiles (Fig. 5B and 5D). A regional difference in G protein coupling has also been noted for D₁ dopamine receptors (Jin et al., 2001). Despite this regional difference, repeated morphine treatment decreased both Gi and Go coupling and again evoked a pronounced Gs coupling. As observed in striatum, NLX co-treatment attenuated the morphine-induced Gs coupling, and profoundly enhanced Gi/o coupling to levels beyond those of vehicle-treated rats.

The alterations in G protein coupling were not due to changes in expression of either MOR or G α proteins (Fig. 6). In addition, MOR was demonstrated to be the unique target of the

anti-MOR antibody since this antibody did not recognize any proteins in striatal tissue from MOR $-/-$ mice (Fig. 7, top panel). As a further control, G protein coupling to the KOR was successfully demonstrated in MOR $-/-$ tissue (Fig. 7, bottom panel).

G protein coupling alterations confirmed by [³H]DAMGO binding

The chronic morphine-induced G protein coupling switch and its attenuation by ultra-low-dose NLX were confirmed

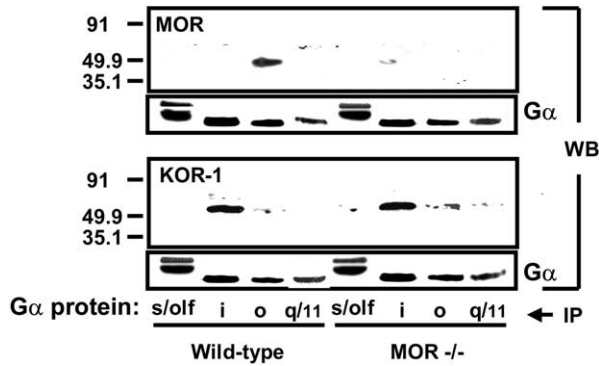


Fig. 7. Specificity of the MOR antibody demonstrated by a lack of detectable MOR coupling to $G\alpha$ proteins in MOR knockout ($-/-$) mice. Immunoprecipitates of $G\alpha$ proteins using specific anti- $G\alpha$ s/olf (s/olf), - $G\alpha$ i (i), - $G\alpha$ o (o) or $G\alpha$ q/11 (q/11) antibodies were probed by Western blotting with antibodies specific to MOR and KOR in striatum of wild-type (WT) and MOR $-/-$ mice. While anti- $G\alpha$ o antibody co-immunoprecipitated MORs in striatal tissue of WT mice, MORs were absent from the anti- $G\alpha$ o immunoprecipitate in MOR $-/-$ mice. In contrast, both WT and MOR $-/-$ mice showed comparable KOR-1 coupling to $G\alpha$ i. The blots were stripped and re-probed with antibodies against various $G\alpha$ proteins, illustrating similar amounts of $G\alpha$ proteins precipitated.

by experiments in which specific [3 H]DAMGO [D-Ala₂, (MePhe)₄, Gly₅-ol]enkephalin binding was employed to quantify MORs in the anti- $G\alpha$ immunoprecipitates derived from spinal cord of vehicle-, morphine- and morphine+NLX-treated rats. The results again show that MOR couples to Go and Gi in opioid-naïve rats, and that chronic morphine treatment induces robust Gs coupling to MOR and a concurrent reduction in the Gi/o coupling (Fig. 8), confirming

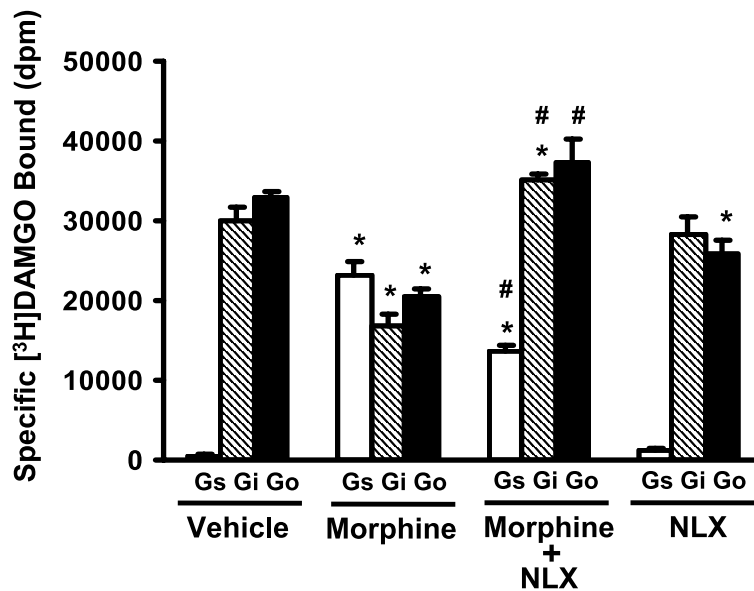


Fig. 8. Specific [3 H]DAMGO binding in anti- $G\alpha$ immunoprecipitates derived from spinal cord of the different treatment groups. [3 H]DAMGO binding confirmed the pattern of G protein coupling shown by co-immunoprecipitation with the anti-MOR antibody shown in Fig. 2. A marked amount of [3 H]DAMGO binding was detected in $G\alpha$ s immunoprecipitates in spinal cord from morphine- but not vehicle-treated rats. In spinal cord from rats treated with morphine+NLX, [3 H]DAMGO binding was decreased in $G\alpha$ s immunoprecipitates compared with the morphine group, and increased in $G\alpha$ i/o immunoprecipitates compared with the vehicle group. Data are means \pm S.E.M. derived from four individual rats in each treatment group that were processed individually ($n=4$). * $P<0.05$ versus same $G\alpha$ protein in vehicle group. # $P<0.05$ versus same $G\alpha$ protein in morphine group.

data obtained using the MOR antibody to identify the receptors Fig. 2. These [3 H]DAMGO binding data also confirm the attenuation of MOR–Gs coupling and the marked enhancement of MOR coupling to Gi/o, to levels higher than in the vehicle group, by co-treatment with ultra-low-dose NLX (Fig. 8). While treatment with 10 ng/kg NLX twice daily for 7 days did not alter the pattern of MOR–G protein coupling, a $21\pm 5\%$ decrease in Go-coupled [3 H]DAMGO was observed (Fig. 8).

[35 S]GTP γ S binding shows similar coupling alterations in PAG

Further evidence that opioid tolerance is associated with the appearance of MOR–Gs coupling was derived from an established [35 S]GTP γ S binding assay used to assess the linkage of receptor to $G\alpha$ proteins (Friedman et al., 1993). MOR coupling to Gi, Go, Gs and Gq was assessed in PAG from the four treatment groups ($n=4$). After *in vitro* stimulation of MOR with the selective agonist DAMGO, the [35 S]GTP γ S-bound $G\alpha$ proteins were immunoprecipitated with specific antibodies against the various $G\alpha$ proteins. The [35 S]GTP γ S in each immunoprecipitate was quantified to reveal the pattern of G protein coupling in PAG of the four treatment groups (Fig. 9). This experiment revealed a coupling pattern similar to that shown via the co-immunoprecipitation technique used with striatum and spinal cord tissue. MOR coupled to both Go and Gi in PAG of vehicle- and NLX-treated rats, and morphine-treated rats showed the emergence of coupling to Gs concurrent with a decrease in coupling to Gi/o proteins was noted. Although NLX alone did not affect the pattern of Gi/o coupling to MORs, this treatment enhanced Gi-MOR association by

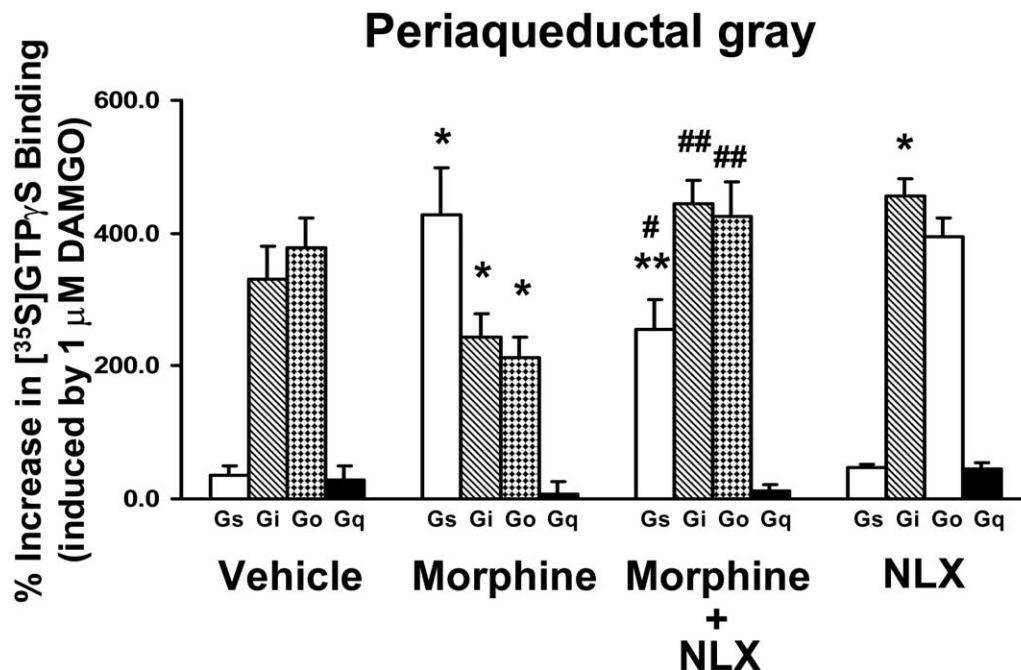


Fig. 9. Chronic morphine treatment induced activation of G α s in PAG that was attenuated by NLX co-treatment, shown here by [³⁵S]GTP γ S binding. Membranes were incubated with 0.5 nM [³⁵S]GTP γ S followed by incubation with vehicle or 1 μ M DAMGO. Membranes were then solubilized and [³⁵S]GTP γ S-bound G α proteins were separately immunoprecipitated using anti-G α antibodies. Data are means \pm S.E.M. obtained from four separate experiments each using a single rat from each treatment group ($n=4$). * $P<0.05$; ** $P<0.01$ versus same G α protein in vehicle group. # $P<0.05$; ## $P<0.01$ versus same G α protein in morphine group.

38 \pm 7%. NLX co-treatment again decreased coupling to Gs and restored coupling to Gi/o to levels slightly above that of vehicle-treated rats. These experiments were also performed using *in vitro* morphine and the results were essentially identical (data not shown).

Ultra-low-dose NLX attenuates G $\beta\gamma$ -adenylyl cyclase interaction

To test whether G $\beta\gamma$ contributes to chronic morphine-associated adenylyl cyclase super-activation, we examined the direct coupling of G $\beta\gamma$ to adenylyl cyclase types II and IV, subtypes known to be regulated by G $\beta\gamma$ (Tang and Gilman, 1991). Striatal and spinal cord membranes from rats of the four treatment groups ($n=4$) were stimulated *in vitro* with DAMGO in the presence of the non-hydrolyzable GTP analog, Gpp(NH)p, which was added to prevent G protein cycling. The G $\beta\gamma$ coupled to adenylyl cyclase II or IV was co-immunoprecipitated with a pan-G β antibody. Western blots of the immunoprecipitates were then sequentially probed with antibody against the type II cyclase and subsequently re-probed with an antibody to adenylyl cyclase type IV. While coupling between G $\beta\gamma$ and the cyclases was not detectable in vehicle-treated tissues, chronic morphine treatment elicited coupling of G $\beta\gamma$ to adenylyl cyclase II and IV in both striatum and spinal cord in response to *in vitro* stimulation with DAMGO (Figs. 10 and 11). This morphine-induced effect was markedly attenuated or abolished by NLX co-treatment as reflected by the reduced levels of adenylyl cyclase types II (Fig. 10) and IV (Fig.

11) in G β immunoprecipitates. In tissues obtained from treatment with NLX alone, no detectable association between G β and the adenylyl cyclases was detected both at baseline and after MOR stimulation. These changes in coupling were not due to treatment-induced changes in expression levels of G β or adenylyl cyclases (Fig. 12).

DISCUSSION

Although excitatory effects of opiates have been implicated in opioid tolerance and dependence, the alterations in MOR signaling that mediate these excitatory effects have not been directly examined, particularly in an *in vivo* treatment paradigm. These data demonstrate chronic morphine-induced MOR signaling alterations and their suppression by the addition of an ultra-low dose of NLX, offering a mechanism for the attenuation of tolerance and dependence by ultra-low-dose opioid antagonists. In addition, the enhanced Gi/o coupling in spinal cord seen in the co-treated animals offers a mechanistic explanation for the enhanced analgesia of these combinations seen even after acute administration (Crain and Shen, 1995).

While the current study examined the behavioral and molecular effects of ultra-low-dose NLX with morphine, these effects may generalize to other combinations of opioid agonists with ultra-low-dose opioid antagonists. Ultra-low-dose naltrexone (10 ng/kg s.c. or 0.05 ng intrathecally) has previously been used *in vivo* with morphine to enhance acute analgesia, to prevent dependence, and to

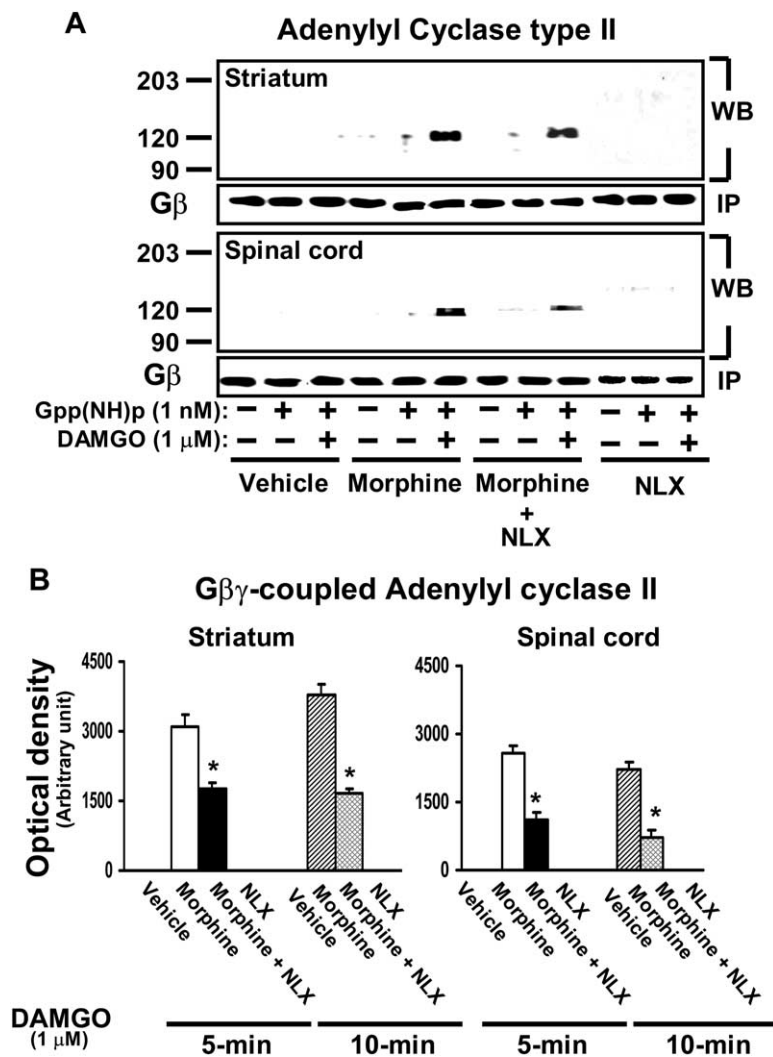


Fig. 10. Chronic morphine treatment caused direct association of Gβγ proteins with adenylyl cyclase type II, shown by co-immunoprecipitation of Gβ proteins with adenylyl cyclase II protein. This morphine-induced Gβγ-adenylyl cyclase II interaction was attenuated by the 10 ng/kg NLX co-treatment. Adenylyl cyclase type II is detected in Western blots of immunoprecipitates of Gβ protein from striatal or spinal cord membranes that were stimulated with DAMGO for 5 min (and not shown, 10 min) in the presence of Gpp(NH)p (A). The blots were stripped and re-probed with an anti-Gβ antibody, demonstrating that equivalent Gβ protein levels were precipitated in each lane. Densitometric quantifications were performed on blots representing 5-min DAMGO incubations as well as those representing 10-min incubations (B). Data are means ± S.E.M. derived from four individual rats in each treatment group that were processed individually ($n=4$). * $P<0.05$ versus morphine group.

prevent or reverse tolerance (Crain and Shen, 1995; Powell et al., 2002; Oxbro et al., 2003). Both NLX and naltrexone have been shown to prevent the excitatory effects of opiates *in vitro* by electrophysiology (Shen and Crain, 1994; Crain and Shen, 1995). Clinically, ultra-low-dose NLX has demonstrated the enhancement of morphine analgesia in an acute intra-operative setting (Hamman et al., 2004) and an opioid-sparing effect for patients on PCA morphine (Gan et al., 1997). Ultra-low-dose naltrexone has also produced profound analgesia in combination with methadone for a severely opioid tolerant patient (Cruciani et al., 2003), and more recently enhanced the analgesia of oxycodone in a large, randomized, placebo- and active-controlled trial (Chindalore et al., 2005). Ultra-low-dose nalmefene has also enhanced morphine analgesia and

reduced the need for antiemetics and antipruritics (Joshi et al., 1999).

The present results directly support the co-existence of two hypotheses of altered MOR signaling in opioid tolerance: a switch in the pattern of G protein coupling to Gs (Crain and Shen, 1998) and a stimulation of adenylyl cyclase by Gβγ (Gintzler and Chakrabarti, 2001). Gintzler and Chakrabarti (2001) suggest that the excitatory signaling by Gβγ to adenylyl cyclase occurs without an alteration in the G protein coupling profile. The virtually identical pattern of treatment effects on Gs coupling as on the Gβγ-adenylyl cyclase interaction shown here suggests that the Gβγ dimer that signals to adenylyl cyclase after chronic morphine originates from the Gs heterotrimer and not from the Gi/o proteins that have reduced their coupling

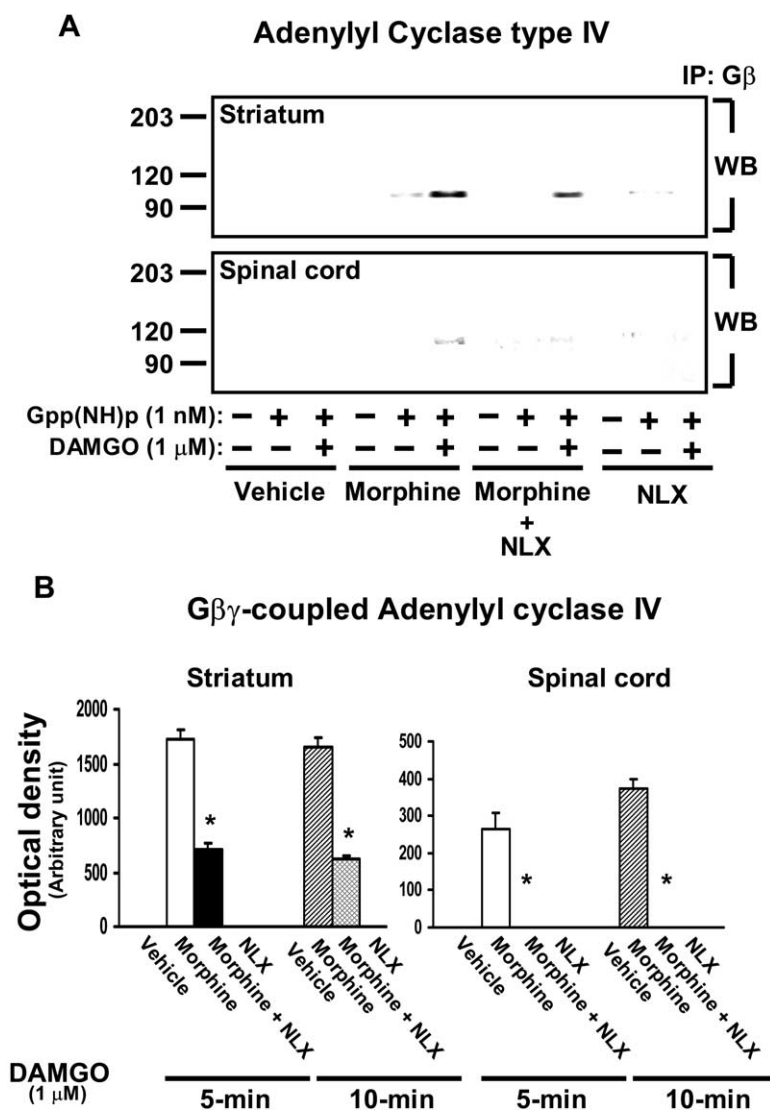


Fig. 11. Chronic morphine treatment also caused direct coupling of G β γ proteins to adenylyl cyclase type IV as shown by co-immunoprecipitation of G β proteins with adenylyl cyclase IV proteins. This morphine-induced G β γ -adenylyl cyclase IV association was also attenuated by the NLX co-treatment. Western blots in Fig. 7A were stripped and re-probed with an antibody to adenylyl cyclase type IV (A). Densitometric quantifications are shown in B. Data are means \pm S.E.M. derived from four individual rats in each treatment group ($n=4$). * $P<0.05$ versus morphine group.

to MOR. The excitatory effect on the cell that occurs during opioid tolerance therefore appears to be an additive or synergistic effect of a loss of adenylyl cyclase inhibition by G α i/o and a stimulation of adenylyl cyclase by both G α s and its associated G β γ . The G β γ associated with Gs coupling to other receptors in diverse cell types has demonstrated a variety of effects, including activation of adenylyl cyclase (Belevych et al., 2001) and GIRKs (Robillard et al., 2000) and inhibition of NADPH oxidase (Krieger-Brauer et al., 2000). The hyperpolarizing effects on the cell via G β γ signaling to ion channels, normally elicited by G β γ dissociating from G α i/o, should also be attenuated when receptor-Gi/o coupling decreases. Moreover, the data presented here imply that G β γ stimulation of adenylyl cyclase types II and IV contributes to an increase in cAMP production which was previously suggested to underlie hyperalgesic or excitatory effects of chronic opiate administration

(Wang and Gintzler, 1997). While the emergence of coupling to Gs would be expected to promote excitatory signaling through G α s, our data suggest that it also induces a G β γ -adenylyl cyclase interaction and that both events may contribute to an enhanced activation of adenylyl cyclase associated with opioid tolerance and dependence.

Our data and the effects of chronic morphine in β -arrestin-2 knockout mice support the notion that MOR desensitization, or a decrease in the native Gi/o coupling, mediates analgesic tolerance. Like the β -arrestin-2 knockout, co-treatment with ultra-low-dose NLX prevented the chronic morphine-induced reduction in intrinsic MOR-Gi/o coupling, maintaining analgesia by continued inhibition of adenylyl cyclase or perhaps merely by the interaction of Gi/o-associated G β γ with ion channels. However, although the β -arrestin-2 knockout prevents MOR desensitization, the activation of adenylyl cyclase in these animals is un-

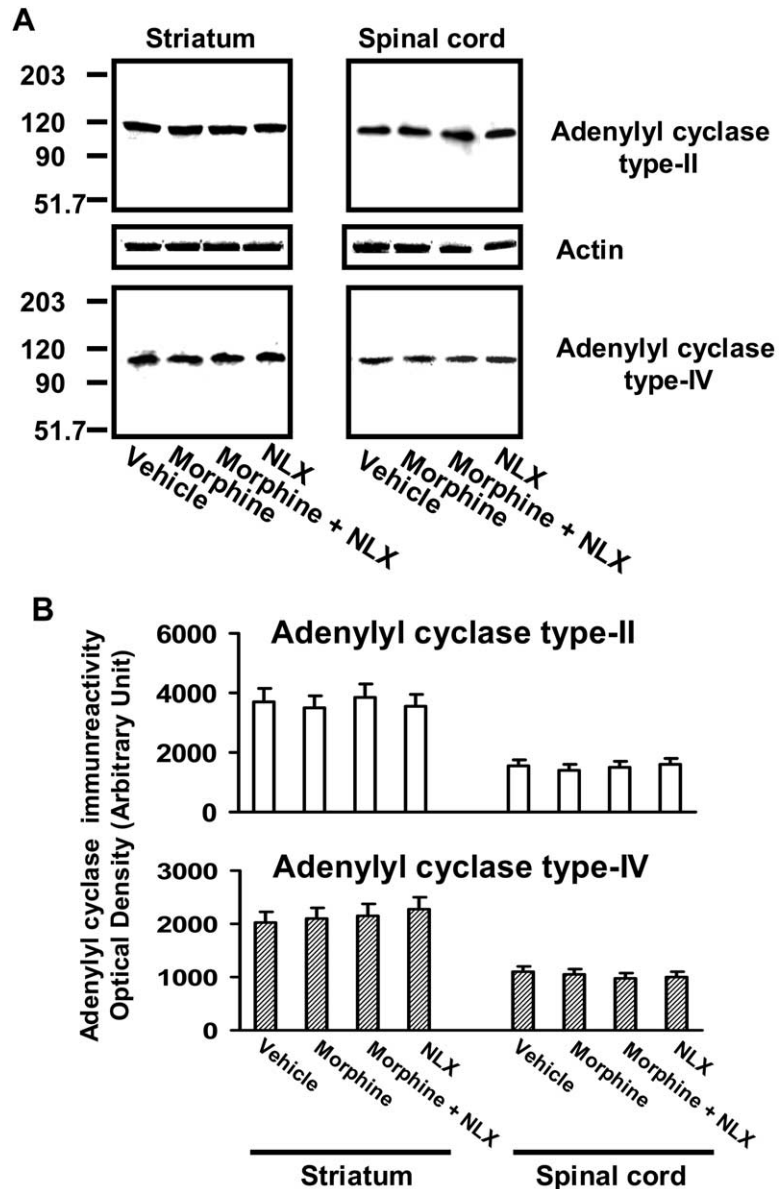


Fig. 12. Western blots comparing the relative levels of adenylyl cyclase type II and IV in the different treatment groups (A). The blots were stripped and re-probed with an anti-actin antibody to determine the actin immunoreactivities as loading controls. Alterations in coupling of $G\beta\gamma$ to adenylyl cyclase type II and IV induced by morphine and alleviated by ultra-low-dose NLX were not due to changes in expression of adenylyl cyclase type II and IV proteins in striatum or spinal cord. Densitometric quantifications of blots are shown in B. Data are means \pm S.E.M. derived from four individual rats from each treatment group that were processed individually ($n=4$).

affected, as is dependence (Bohn et al., 2000). Hence, the morphine-induced activation of adenylyl cyclase appears to mediate dependence in the β -arrestin-2 knockout mice, and this activation might be the result of G_s coupling that occurs despite a lack of G_i/o desensitization. This possibility suggests that chronic morphine might not cause a simple coupling switch in a given receptor, but possibly, a change in the probability of signaling by one receptor population versus another. Ultra-low-dose NLX's attenuation of MOR- G_s coupling, concurrent with a restoration of MOR- G_i/o coupling, may explain its attenuation of both tolerance and dependence.

Two other examples of a G protein coupling switch by receptors have been reported, although the concept is still controversial. The β_2 -adrenergic receptor can switch from G_s to G_i coupling, and this switch also leads to altered signaling by both $G\beta\gamma$ and the α subunit novel to this receptor, leading to different signaling cascades (Daaka et al., 1997). In this case, protein kinase A-mediated phosphorylation of the receptor reduces coupling efficiency to G_s and enhances coupling efficiency to G_i , thus enabling activation of MAPK via $G\beta\gamma$. The second example is the CB_1 cannabinoid receptor, which normally couples to G_i/o . Here, concurrent activation of D_2 dopamine receptors with

CB₁ receptors causes a shift in coupling of the CB₁ receptor to G_s, resulting in accumulation rather than inhibition of cAMP (Jarrahian et al., 2004). The CB₁ receptor was also shown to switch G protein coupling following pertussis toxin treatment, which ADP-ribosylates G α i/o resulting in dissociation of the Gi/o trimer, thereby preventing its interaction with the receptor and enabling coupling to G_s (Bonhaus et al., 1998).

A common theme in all these examples of a change in the G protein coupling profile is the loss of coupling efficiency to the original G protein. After chronic agonist exposure, opioid receptors desensitize via phosphorylation by G-protein receptor kinases and subsequent binding by the regulatory proteins β -arrestins that in turn reduce the efficiency of intrinsic Gi/o protein coupling (Ferguson et al., 1996). The novel association of MOR with G_s may be due to receptor modifications caused by repeated stimulation such as altering the phosphorylation state of the receptor or the G protein that in turn leads to a change in coupling efficiency. Alternatively, continued signaling and recycling of receptor and G proteins during prolonged morphine exposure may result in regrouping of MOR, G proteins, effectors and regulatory molecules that facilitate the novel interactions merely by variations in proximities among these membrane constituents.

This paper confirms the earlier hypothesis that ultra-low-dose opioid antagonists antagonize excitatory functions of opioid receptors (Crain and Shen, 2000). However, the mechanism by which opioid antagonists attenuate the cellular adaptations shown here at such exceedingly low doses is not yet fully understood. Clearly, higher doses of an opioid antagonist would prevent opioid tolerance but these doses would also prevent the activity of the opiate. In the Powell et al. (2002) study, 10 ng/kg of naltrexone more potently reversed morphine tolerance than did 50 ng/kg. In an earlier study, 100 ng/kg naltrexone was more effective at enhancing the acute antinociceptive potency of morphine than either 1 μ g/kg or 1 ng/kg naltrexone (Shen and Crain, 1997). Although NLX and naltrexone have been shown to act as inverse agonists at MOR after chronic opioid exposure (Wang et al., 2004a), such blockade of basal signaling by uncoupling MORs from their native G proteins (Gi/o) does not explain the present finding that ultra-low-dose NLX suppressed G_s coupling while *enhancing* Gi/o coupling. An inverse agonist would uncouple the receptor from all G proteins. Moreover, our results clearly demonstrate that NLX at 10 ng/kg itself has little effect on MOR or its associated signaling components in the absence of the opiate. This result is consistent with our finding that ultra-low-dose NLX alone did not affect nociception here, nor did ultra-low-dose naltrexone previously (Crain and Shen, 1995). The subtle NLX-induced change in the ratio of Gi to Go coupling detected by [³H]DAMGO and [³⁵S]GTP γ S binding may simply reflect the noise of these assays without functional implications, especially since vehicle and NLX groups did not differ in the co-immunoprecipitation assay. Collectively, these data suggest that ultra-low-dose NLX co-treatment may enhance the ability of MOR or MOR-associated protein complexes

to resist re-alignment induced by chronic exposure to MOR agonists.

Using saturation binding studies (Lewanowitsch and Irvine, 2003) the estimated receptor occupancy of a similar dose of NLX is about 1% of the MOR population if one assumes 100% CNS availability. It is possible that MORs coupling to G_s differentially alter NLX and morphine dissociation rates since the slow dissociation phase of a NLX analog (NLX benzoylhydrazone) from MOR was eliminated by pertussis toxin, which targets Gi/o, but not by cholera toxin, which targets G_s (Brown and Pasternak, 1988). By this reasoning, repeated morphine exposure might alter the receptor in a way that reduces its affinity for Gi/o proteins, promotes coupling to G_s and enhances its relative affinity for NLX. Although such a change in affinity of a sub-population of receptors may not feasibly explain ultra-low-dose NLX's mechanism of attenuating tolerance and dependence, the shift in G protein coupling profiles is clearly governed by factors highly sensitive to NLX. The fact that the time-effect curve for NLX in blocking opioid analgesia is shorter than the time-effect curve for morphine in inducing analgesia suggests a novel target for ultra-low-dose NLX in these effects. Potential targets of ultra-low-dose opioid antagonists on these receptors include changes in receptor conformation and associated membrane proteins. Such targets become more feasible if they simultaneously affect the coupling of multiple MORs. Moreover, although receptor changes that may alter MOR signaling are not yet elucidated, the present results more clearly define the mechanism of ultra-low-dose opioid antagonists in blocking excitatory signaling of opioid receptors and potentially in enhancing analgesia and preventing tolerance and withdrawal (Crain and Shen, 1995; Powell et al., 2002).

The present work showed that ultra-low-dose NLX co-treatment attenuates chronic morphine-induced MOR signaling alterations as well as morphine analgesic tolerance and dependence. Clinically, ultra-low-dose naltrexone combined with oxycodone (Oxytrex™) was recently shown to produce significantly greater pain relief than the same dose of oxycodone administered alone in a randomized, double-blind, placebo-controlled, 350-patient clinical trial of osteoarthritis patients (Chindalore et al., 2005). In addition, a longer, phase III clinical trial of Oxytrex demonstrated equivalent analgesia from a significantly lower dose of oxycodone when combined with ultra-low-dose naltrexone than from oxycodone alone. The addition of ultra-low-dose naltrexone in this phase III clinical trial also dramatically reduced opioid dependence as measured by the short opioid withdrawal scale following abrupt cessation of treatment (Webster, manuscript in preparation). Recent preclinical data using environmental conditioning paradigms showed that ultra-low-dose naltrexone co-treatment reduced the aversive effects of opioid withdrawal and also the acute rewarding or "euphoric" effects of opiates (Olmstead and Burns, 2005). Additionally, ultra-low-dose naltrexone was shown to reduce the rewarding potency of oxycodone and subsequent "drug-seeking" in a rat model of addiction (Leri and Burns, *in press*). In summary, ultra-

low-dose opioid antagonists appear to alleviate a variety of undesirable effects of opioids, and the attenuation of chronic morphine-induced signaling alterations shown here suggests an underlying molecular mechanism.

Acknowledgments—We thank Bridgitte Kieffer for the use of MOR $-/-$ tissue, and we thank Chris Evans for providing this tissue and for his insightful comments in the early preparation of this manuscript. We also acknowledge the excellent technical assistance of Kalindi Bakshi (molecular pharmacology experiments) and Jay Paquette and Amanda Green (behavioral experiments). This work was funded by Pain Therapeutics, Inc.

REFERENCES

- Arner S, Rawal N, Gustafsson LL (1988) Clinical experience of long-term treatment with epidural and intrathecal opioids: a nationwide survey. *Acta Anaesthesiol Scand* 32:253–259.
- Avidor-Reiss T, Bayewitch M, Levy R, Matus-Leibovitch N, Nevo I, Vogel Z (1995) Adenylyl cyclase supersensitization in mu-opioid receptor-transfected Chinese hamster ovary cells following chronic opioid treatment. *J Biol Chem* 270:29732–29738.
- Belevych AE, Sims C, Harvey RD (2001) ACh-induced rebound stimulation of L-type Ca^{2+} current in guinea-pig ventricular myocytes, mediated by Gbetagamma-dependent activation of adenylyl cyclase. *J Physiol* 536:677–692.
- Bohn LM, Gainetdinov RR, Lin FT, Lefkowitz RJ, Caron MG (2000) Mu-opioid receptor desensitization by beta-arrestin-2 determines morphine tolerance but not dependence. *Nature* 408:720–723.
- Bonhaus DW, Chang LK, Kwan J, Martin GR (1998) Dual activation and inhibition of adenylyl cyclase by cannabinoid receptor agonists: Evidence for agonist-specific trafficking of intracellular responses. *J Pharmacol Exp Ther* 287:884–888.
- Brown GP, Pasternak GW (1988) 3H -naloxone benzoylhydrazone binding in MOR-1 transfected Chinese hamster ovary cells: Evidence for G-protein-dependent antagonist binding. *J Pharmacol Exp Ther* 268:376–381.
- Chen C, Xue JC, Zhu J, Chen YW, Kunapuli S, de Riel JK, Yu L, Liu-Chen LY (1995) Characterization of irreversible β -funaltrexamine binding to the cloned rat μ -opioid receptor. *J Biol Chem* 270:17866–17870.
- Chindalore VL, Craven RA, Butera PG, Yu KP, Burns LH, Friedmann N (2005) Adding ultra-low-dose naltrexone to oxycodone enhances and prolongs analgesia. *J Pain* 6:392–399.
- Connor M, Christie MD (1999) Opioid receptor signalling mechanisms. *Clin Exp Pharmacol Physiol* 26:493–499.
- Crain SM, Shen K-F (1990) Opioids can evoke direct receptor-mediated excitatory effects on sensory neurons. *Trends Pharmacol Sci* 11:77–81.
- Crain SM, Shen K-F (1992) After chronic opioid exposure sensory neurons become supersensitive to the excitatory effects of opioid agonists and antagonists as occurs after acute elevation of GM1 ganglioside. *Brain Res* 575:13–24.
- Crain SM, Shen K-F (1995) Ultra-low concentrations of naloxone selectively antagonize excitatory effects of morphine on sensory neurons, thereby increasing its antinociceptive potency and attenuating tolerance/dependence during chronic cotreatment. *Proc Natl Acad Sci U S A* 92:10540–10544.
- Crain SM, Shen K-F (1998) Modulation of opioid analgesia, tolerance and dependence by Gs-coupled, GM1 ganglioside-regulated opioid receptor functions. *Trends Pharmacol Sci* 19:358–365.
- Crain SM, Shen K-F (2000) Antagonists of excitatory opioid receptor functions enhance morphine's analgesic potency and attenuate opioid tolerance/dependence liability. *Pain* 84:121–131.
- Crain SM, Shen K-F (2001) Acute thermal hyperalgesia elicited by low-dose morphine in normal mice is blocked by ultra-low-dose naltrexone, unmasking potent opioid analgesia. *Brain Res* 888:75–82.
- Cruciani RA, Lussier D, Miller-Saultz D, Arbuck DM (2003) Ultra-low dose oral naltrexone decreases side effects and potentiates the effect of methadone. *J Pain Symptom Manage* 25:491–494.
- Daaka Y, Luttrell LM, Lefkowitz RJ (1997) Switching of the coupling of the beta2-adrenergic receptor to different G proteins by protein kinase A. *Nature* 390:88–91.
- Federman AD, Conklin BR, Schrader KA, Reed RR, Bourne HR (1992) Hormonal stimulation of adenylyl cyclase through Gi-protein beta gamma subunits. *Nature* 356:159–161.
- Ferguson SS, Barak LS, Zhang J, Caron MG (1996) G-protein-coupled receptor regulation: role of G-protein-coupled receptor kinases and arrestins. *Can J Physiol Pharmacol* 74:1095–1110.
- Friedman E, Butkerait P, Wang H-Y (1993) Analysis of receptor-stimulated and basal guanine nucleotide binding to membrane G proteins by sodium dodecyl sulfate-polyacrylamide gel electrophoresis. *Anal Biochem* 214:171–178.
- Friedman E, Wang H-Y (1996) Receptor-mediated activation of G proteins is increased in postmortem brains of bipolar affective disorder subjects. *J Neurochem* 67:1145–1152.
- Gan TJ, Ginsberg B, Glass PSA, Fortney J, Jhaveri R, Perno R (1997) Opioid-sparing effects of a low-dose infusion of naloxone in patient-administered morphine sulfate. *Anesthesiology* 87:1075–1081.
- Gintzler AR, Chakrabarti S (2001) Opioid tolerance and the emergence of new opioid receptor-coupled signaling. *Mol Neurobiol* 21:21–33.
- Hamman S, Wala E, Rebel A, Lock R (2004) Selective antagonism of excitatory opioid receptor systems: A pilot clinical study demonstrating enhancement of morphine analgesia by low-dose naloxone in female patients undergoing elective laparotomy. *Proceedings of the American Society of Anesthesiologists*, New Orleans, LA.
- Ikeda K, Kobayashi T, Kumanishi T, Niki H, RY (2000) Involvement of G-protein-activated inwardly rectifying K^{+} (GIRK) channels in opioid-induced analgesia. *Neurosci Res* 38:113–116.
- Jarrahan A, Watts VJ, Barker EL (2004) D2 dopamine receptors modulate G_{α} -subunit coupling of the CB1 cannabinoid receptor. *J Pharmacol Exp Ther* 308:880–886.
- Jin LQ, Wang H-Y, Friedman E (2001) Stimulated D(1) dopamine receptors couple to multiple Galpha proteins in different brain regions. *J Neurochem* 78:981–990.
- Joshi GP, Duffy L, Chehade J, Wesevich J, Gajraj N, Johnson ER (1999) Effects of prophylactic nalmeferene on the incidence of morphine-related side effects in patients receiving intravenous patient-controlled analgesia. *Anesthesiology* 90:1007–1011.
- Kayser V, Besson JM, Guilbaud G (1987) Paradoxical hyperalgesic effect of exceedingly low doses of systemic morphine in an animal model of persistent pain (Freund's adjuvant-induced arthritis rats). *Brain Res* 414:155–157.
- Kiyatkin EA (1989) Morphine: some puzzles of a well-known substance. *Int J Neurosci* 45:231–246.
- Krieger-Brauer HI, Medda P, Kather H (2000) Basic fibroblast growth factor utilizes both types of component subunits of Gs for dual signaling in human adipocytes. Stimulation of adenylyl cyclase via Galph(s) and inhibition of NADPH oxidase by Gbeta gamma(s). *J Biol Chem* 275:35920–35925.
- Laugwitz KL, Offermanns S, Spicher K, Schultz G (1993) Mu and delta opioid receptors differentially couple to G protein subtypes in membranes of human neuroblastoma SH-SY5Y cells. *Neuron* 10:233–242.
- Leri F, Burns LH (2005) Ultra-low-dose naltrexone reduces rewarding potency of oxycodone and relapse vulnerability in rats. *Pharmacol Biochem Behav*, in press.
- Lewanowitsch T, Irvine RJ (2003) Naloxone and its quaternary derivative, naloxone methiodide, have differing affinities for mu, delta, kappa opioid receptors in mouse brain homogenates. *Brain Res* 964:302–305.

- MacRae J, Siegel S (1997) The role of self-administration in morphine withdrawal in rats. *Psychobiology* 25:77–82.
- Nestler EJ (2001) Molecular neurobiology of addiction. *Am J Addict* 10:201–217.
- Olmstead MC, Burns LH (2005) Ultra-low-dose naltrexone suppresses rewarding effects of opiates and aversive effects of opiate withdrawal in rats. *Psychopharmacology*, in press.
- Oxbro K, Trang T, Sutak M, Jhamandas KH (2003) The effects of spinal ultra-low doses of an opioid receptor antagonist on systemic morphine dependence. *Proceedings of the Society for Neuroscience*, New Orleans, LA.
- Powell KJ, Abul-Husn NS, Jhamandas A, Olmstead MC, Beninger RJ, Jhamandas K (2002) Paradoxical effects of the opioid antagonist naltrexone on morphine analgesia, tolerance, and reward in rats. *J Pharmacol Exp Ther* 300:588–596.
- Robillard L, Ethier N, Lachance M, Hebert TE (2000) Gbetagamma subunit combinations differentially modulate receptor and effector coupling in vivo. *Cell Signal* 12:673–682.
- Saegusa H, Kurihara T, Zong S, Minowa O, Kazuno A, Han W, Matsuda Y, Yamanaka H, Osanai M, Noda T, Tanabe T (2000) Altered pain responses in mice lacking $\alpha 1E$ subunit of the voltage-dependent Ca^{2+} channel. *Proc Natl Acad Sci U S A* 97: 6132–6137.
- Shen KF, Crain SM (1989) Dual opioid modulation of the action potential duration of mouse dorsal root ganglion neurons in culture. *Brain Res* 491:227–242.
- Shen KF, Crain SM (1994) Antagonists at excitatory opioid receptors on sensory neurons in culture increase potency and specificity of opiate analgesics and attenuate development of tolerance/dependence. *Brain Res* 636:286–297.
- Shen KF, Crain SM (1997) Ultra-low doses of naltrexone or etorphine increase morphine's antinociceptive potency and attenuate tolerance/dependence in mice. *Brain Res* 757:176–190.
- Shen K-F, Crain SM (1990) Cholera toxin-A subunit blocks opioid excitatory effects on sensory neuron action potentials indicating mediation by Gs-linked opioid receptors. *Brain Res* 525:225–231.
- Tang W-J, Gilman AG (1991) Type specific regulation of adenylyl cyclase by G protein beta gamma subunits. *Science* 254: 1500–1503.
- Vanderah T, Ossipov M, Lai J, Malan T, Porreca F (2001) Mechanisms of opioid-induced pain and antinociceptive tolerance: descending facilitation and spinal dynorphin. *Pain* 92:5–9.
- Veerman E, Ligtenberg A, Schenkels L, Walgreen-Weterings E, Nieuw Amerongen A (1995) Binding of human high-molecular-weight salivary mucins (MG1) to Hemophilus parainfluenzae. *J Dent Res* 74: 351–357.
- Wang D, Raehal KM, Lin ET, Lowery JJ, Kieffer BL, Bilsky EJ, Sadee W (2004a) Basal signaling activity of mu opioid receptor in mouse brain: Role in narcotic dependence. *J Pharmacol Exp Ther* 308: 512–520.
- Wang H-Y, Burns LH, Friedman E (2004b) Ultra-low-dose naloxone suppresses tolerance-associated alterations in Mu opioid receptor signaling and conformation. *Proceedings of the Society for Neuroscience*, San Diego, CA.
- Wang L, Gintzler AR (1997) Altered mu-opiate receptor-G protein signal transduction following chronic morphine exposure. *J Neurochem* 68:248–254.
- Yamamoto T, Ohno M, Ueki S (1988) A selective-opioid agonist, U-50, 488H, blocks the development of tolerance to morphine analgesia in rats. *Eur J Pharmacol* 156:173–176.
- Yoshimura M, Wu PH, Hoffman PL, Tabakoff B (2000) Overexpression of type 7 adenylyl cyclase in the mouse brain enhances acute and chronic actions of morphine. *Mol Pharmacol* 58:1011–1016.

(Accepted 1 June 2005)
(Available online 5 August 2005)